International Forum on Aeroelasticity and Structural Dynamics
IFASD 2017
25-28 June 2017, Como - Italy

FROM MODEL TO MANUFACTURE: ADDITIVE AEROELASTIC MORPHING TESTBEDS

Alexander M. Pankonien[1], James O. Hardin[2], Nitin Bhagat[3], Gregory W. Reich[4], and John D. Berrigan[5]

[1] Multidisciplinary Science Technology Center, Air Force Research Laboratory
2210 Eighth Street, WPAFB, OH, 45433, USA
alexander.pankonien.ctr@us.af.mil

[2] Soft Matter Materials Branch, Air Force Research Laboratory and UES Inc.
4401 Dayton Xenia Rd., Beavercreek, OH, 45432, USA
james.hardin.8.ctr@us.af.mil

[3] University of Dayton Research Institute
300 College Park, Dayton, OH, USA
nbhagat1@udayton.edu

[4] Multidisciplinary Science Technology Center, Air Force Research Laboratory
2210 Eighth Street, WPAFB, OH, 45433, USA
gregory.reich.1@us.af.mil

[5] Soft Matter Materials Branch, Air Force Research Laboratory
2977 Hobson Way, WPAFB, OH, 45433, USA
john.berrigan.1@us.af.mil

Keywords: morphing, topology, additive, stretchable, sensing, fabrication

Abstract: 3D-printing has enabled a new paradigm for the creation and testing of aeroelastic wind-tunnel testbeds with conventional rib/spar structural topologies that can produce complex coupled effects, such as flutter, within the speed constraints of conventional low-speed wind tunnels. This work focuses on the extension of additive manufacturing to enable non-conventional structural wing topologies such as those that leverage bio-mimetic, distributed sensing and actuation schemes. The tractability of complex topologies via additive processes is demonstrated by the development and fabrication of a morphing trailing edge control surface. This demonstrator utilizes a mixture of material moduli and geometric featuring to balance the appropriate control of stiffness with topological simplicity. The capability of automated additive processes is further shown to enable additional novel features such as arbitrary placement of integrated, stretchable conductors without radically increasing fabrication complexity. This wiring technique eliminates non-linear mechanical contact and attachment problems, which could limit the fidelity of dynamic models when actuating and sensing are incorporated within these testbeds. Finally, the potential impact of these processes on realizable morphing-wing designs driven by analysis is illustrated via parametric variation and production of variations of the demonstrator via a scripted geometric framework.

1 INTRODUCTION

Additive technologies for the fabrication of aerospace-grade structural components have existed for decades in the form of composite lay-ups, injection molding, and similar technologies. Automated techniques for cutting and forming, *i.e.* finishing, additively-produced parts have permitted precise and rapid fabrication of aerospace-grade components. Recently, the emergence of automated additive techniques that enable selective volume fusion (i.e. 3D printers) have expanded the realm of feasible component design as an alternative to traditional subtractive techniques and the associated tooling constraints from the fabrication process [1]. Within this additive-only framework, techniques have targeted polymeric systems, composites, and metals. In the case of metal components produced by Selective Laser Sintering, several additive-only fabricated components have even replaced non load-bearing, conventionally-fabricated components on production aircraft. Beyond the replacement of existing components, when appropriately leveraged for the construction of structural features, 3D-printing can enable new techniques that aid parametric investigation of various complex structural phenomena, such as the optimal kinematic distribution of work [2] or passive broadband vibration suppression [3].

Despite these advances, the use of additive manufacturing for the fabrication of structural components in high-risk, limited-use testbeds has been practically non-existent. In part this is because the traditional fabrication techniques, such as precise machining of beams, were sufficient for the production of single-design testbeds designed with similitude to existing flight vehicles. However, when experimentally investigating potential aeroelastic flight vehicle designs within the design/analysis iteration-loop, the cost for iterative fabrication and testing becomes significantly higher and potentially prohibitive without rapid, precise fabrication techniques [4]. This fabrication barrier-to-entry for experimental testing stands in contrast to developments in multidisciplinary design optimization of aircraft where parametric descriptions of complex designs and ever-increasing computational power are leveraged for rapid, iterative simulated testing of new concepts.

The field of aeroelastic demonstrators is thus a suitable application for additive fabrication in that complex topologies, not previously realizable through conventional techniques, can be rapidly produced and iterated. These techniques can then complement the process of multidisciplinary optimization via iterative checks on parametric changes in design. It is to this realm of rapid iteration between model and experiment that the following work seeks to contribute by demonstration of the design possibilities enabled via additive techniques. Specifically, the work explores an additively-produced non-conventional topology for the control surface on an aeroelastic demonstrator, and additive solutions to its associated integration challenges.

1.1 Additively-produced aeroelastic demonstrators

The development of the demonstrator control surface in this work is motivated by recent efforts by Pankonien *et al.* 2017 [5] to create a completely additively-manufactured flutter demonstrator for investigation of flutter suppression techniques within a low-speed wind tunnel, as shown below in Figure 1. Constructed via the Polyjet process [6], involving selectable mixtures of “hard” and “soft” polymers, the bending and torsional natural frequencies were precisely tailored via geometric distribution to achieve flutter. This work introduced the concept of interpenetrating connective features which permitted constant mass and stiffness design construction without added fasteners. Additionally, the design utilized elastomeric breaks to

alter stiffness within the conventional spar box similar to control surfaces, aiding intuitive comparison with conventional wing structural designs.

Although novel in its ability to demonstrate the approximate scaling of structural stiffness necessary to achieve flutter without resorting to a conventional composite or metallic "strongback" to support an outer mold line of plastic components, the design utilized another aspect of conventional, uniform construction methodology. Specifically, the load-bearing structural elements within the design were all selected to be a single material, creating a conventional rib/sparbox topology. Additionally, the model contained no on-board wiring, instrumentation or actuation mechanisms (*i.e.* control surfaces).

1.2 Scope of the current investigation

This work expands on the previous flutter model that demonstrated 3D-printing as a tool for creating tailorable structures with traditional rib/sparbox topologies to also include non-traditional topologies with selective compliance, enabling complex geometry changes, *i.e.* morphing. To demonstrate this concept, a trailing edge control surface is developed, targeting the locations shown in Figure 1, by selectively tailoring structural properties through both geometry and material selection. Integration challenges associated with stretchable topologies including wiring to arbitrarily distributed actuation and sensing are addressed with a similar additive mindset without significantly increasing fabrication complexity. Finally, the tractability of this additive methodology in realizing parametrically-optimized designs is shown via illustration of how changing a very limited set of parameters can accommodate large changes in performance.

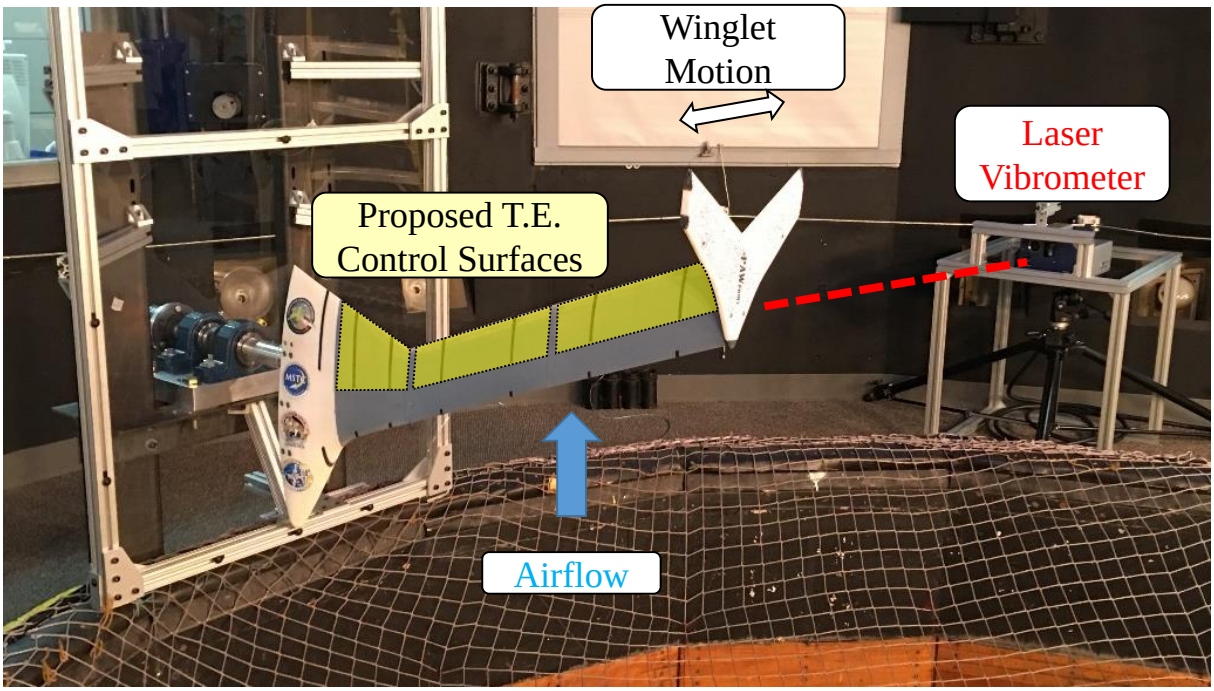

Figure 1: The 3D-printed flutter model as tested in the Vertical Wind Tunnel with the proposed trailing edge control surface locations.

2 DESCRIPTION OF CONTROL SURFACE

A morphing trailing edge control surface represented an ideal target for additive construction methodology for several reasons. First, trailing edge control surfaces have slowly varying geometry due to the near-planar construction of trailing edges creating an approximate 2D interpretation of a complex 3D problem. Second, for demonstration of additive techniques on a non-conventional topology, a tractable problem was needed that necessitated complex stiffness control (and thus topology) with only a few parameters. Typically, morphing control surfaces are described by only a few parameters that represent a complete description of the expected geometry change. Clearly though, more complex topological descriptions were possible.

Targeting a re-interpretation of an existing morphing trailing edge concept for implementation of additive construction with distributed sensing and actuation, the MELD concept by Woods *et al.* 2016 was selected [7]. This transition concept, shown in Figure 2a, permitted smooth trailing edge variation from a fixed rib to a 2D camber morphing concept (the FishBAC [8]) via a set of midline-thickness corrugated ribs. The corrugation angle at each rib was tailored to meet the desired bend-twist coupling at each spanwise station to achieve the smooth trailing edge and bending control surface boundary requirement. A marked advantage of this concept was the simplistic parameterization (the corrugation skew angle) which drove the bend-twist coupling. Disadvantageously, the formulation ignored the spanwise coupling between the ribs, from either skin effects or other mechanisms, which was inherent to the 2D simplification of the problem, requiring the use of an unmodeled corrugated strip to tailor the coupling.

a)

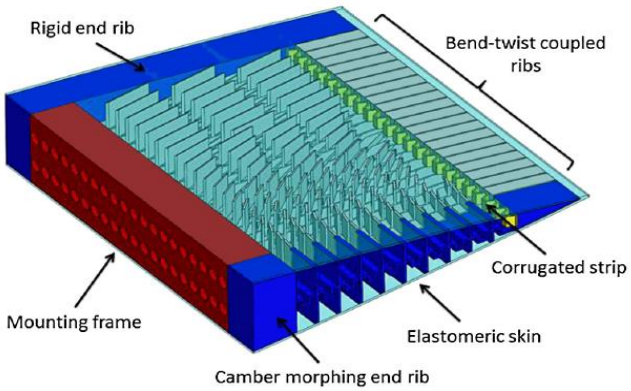

b)

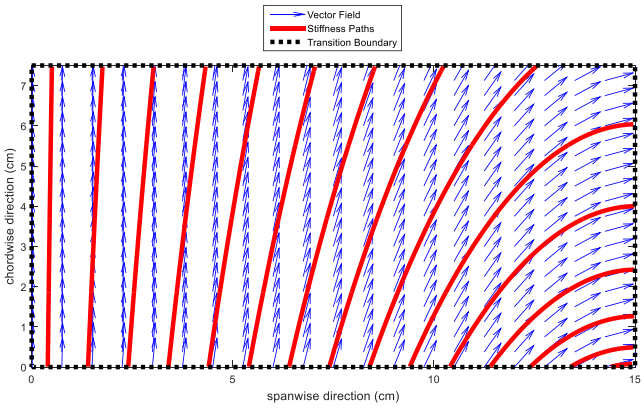

Figure 2: The a) Morphing Elastic Lofted transition from Woods *et al.* 2016 can be deconstructed into its stiffness paths derived from the corrugation skew angles.

2.1 Topology concept- additively integrated skin with reduced geometric complexity

To restore the spanwise (i.e. 3D) coupling effects in a parametric manner, a generalization of the MELD concept to its inherent stiffness performance was necessary. Whereas the MELD concept effectively altered the local skew angle (spanwise) to meet an assumed contour profile via a highly anisotropic geometric feature (midline corrugation), the same contoured profile could be achieved via other anisotropic stiffness-steering features. For example, stiff features could be aligned along to the corrugation's stiff direction in the MELD, via the skew angle. Then, normal to this direction, a compliant feature would be drawn. From a top-down planar perspective, seen in Figure 2b, connecting the stiff features would result in curvilinear SpaRib-like [9] features. These spines resemble ribs near the fixed-rib boundary condition but spars near the bending boundary condition.

Interpreting this top down topology within the context of an additive framework, the Multi-material additively-Integrated Skin Topological Concept for a Morphing Elastic Lofted transition (MISTC-MELD) is generated, as shown via its parametrization in Figure 3. In this parameterization the parameters are selected to be representative of the scale expected for the aeroelastic demonstrator. The spines in the context of 3D geometry become I-beams with defined widths as derived from the trailing edge interior volume and finite skin thickness. The location of the spines are derived via numerical integration from seed-points along the trailing edge, which are evenly spaced in this example but could utilize arbitrary spacing. The compliance and coupling between spines is derived from the distance between the spines and the material properties of compliant skin within this space, rather than mid-plane stiffness control in the original MELD concept. Within the context of multi-material 3D printing, these material properties can be independently selected over a large range of desired performance, including plastic and elastomer.

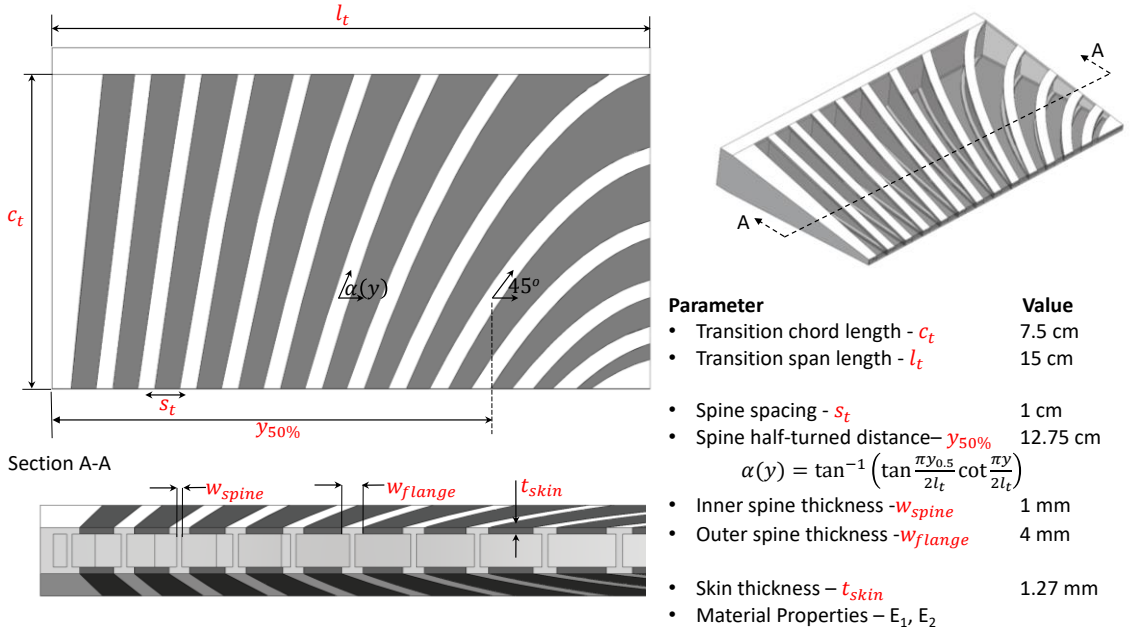

Parameter	Value
• Transition chord length - c_t	7.5 cm
• Transition span length - l_t	15 cm
• Spine spacing - s_t	1 cm
• Spine half-turned distance– $y_{50\%}$	12.75 cm
$\alpha(y) = \tan^{-1}\left(\tan\frac{\pi y_{0.5}}{2l_t}\cot\frac{\pi y}{2l_t}\right)$	
• Inner spine thickness -w_{spine}	1 mm
• Outer spine thickness -w_{flange}	4 mm
• Skin thickness – t_{skin}	1.27 mm
• Material Properties – E_1, E_2	

Figure 3: The Multi-material additively-Integrated Skin Topological Concept for Morphing Elastic Lofted transition (MISTC-MELD) is parameterized with representative values.

Optimizing the stiffness distribution of the MISTC-MELD is inherently a much more complex problem than the original MELD design in that bend-twist coupling performance cannot be optimized via skew angle alone without impacting mass or the skin of the section. However, much more complex contour profiles of the trailing edge, potentially driven by flow analysis, can be described by these parameters, especially if the skew angle is generalized to vary with chordwise as well as spanwise location. Additionally, the corrugation feature is replaced by a less geometrically-complex transition in material properties, which shows greater robustness in turning over the range of 90 degrees.

2.2 Wiring concept- integrated channels for stretchable conductors

Targeting aeroelastic testbeds with diverse sensing requirements, it was assumed that actuators and sensors and appropriate wiring would be needed within the transition region of the control surface. Embedded wires were desired to prevent nonlinear contact phenomena from impacting the dynamics of optimized aeroelastic models. However, traditional metal wires could restrict the actuation of the transition section. Also, it was desired to minimize fabrication complexity to maintain low iteration-cycle time with these aeroelastic demonstrators. Thus, a guided stretchable conductor concept was desired for both actuation and sensing needs.

Although use of a second direct-write machine for the integration of wiring was possible, it would also increase fabrication time and complexity. A methodology for placing these conductors within the constraints of a single 3D printer was needed. Examining stretchable conductor technology, casting custom wiring paths from an elastomeric conductor represented the greatest flexibility in wiring pattern and conductivity. Utilizing a liquid suspension consisting of: silver flakes, TPU, and solvent, stretchable conductors could be cast as a liquid into channels designed into a printed structure and then dried and cleaned to form isolated conductors. As seen in Figure 4, the stretchable conductors could readily interface with traditional electrical components via integrated terminal blocks while crossing an elastomeric section (shown in black) undergoing >30% compressive and tensile strain while remaining conductive.

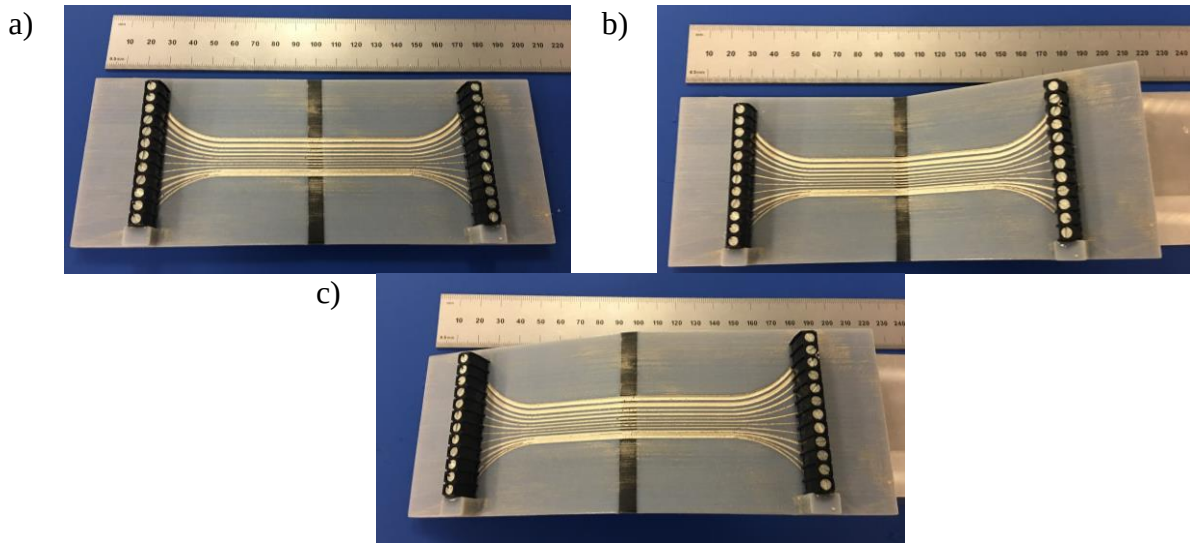

Figure 4: The stretchable conductors cast into channels across an a) elastomeric interface and are capable of b) compression and c) tension strain greater than 30%.

The sizing of the channels was limited only by the resolution of the original 3D printer, which was found to be as small as 0.2 mm deep, 0.4 mm wide, and 0.2 mm apart for a planar surface. The task of wiping the surface clean of the conductive liquid prior could also limit the resolution of isolated conductors while impacting fabrication time. Choosing a low user-intensity methodology, cleaning was performed via a straight-edge covered in cloth, wetted by an acetone-water mixture. After empirically testing several channel sizing parameters, a depth of 400 microns, width of 1 mm, and spacing of 1 mm was selected as an easily reproducible configuration that produced low resistivity. Experimentally, the conductivity was measured at roughly 1,000 S/cm, which was more than sufficient for the 100 KΩ nominal resistance of relevant sensors, described in Section 3.1, or low-power electronics.

There are many advantages to this methodology of wiring, including: elimination of nonlinear mechanical contact phenomena, reduced wire stiffness contribution to elastomeric joints, and wire placement that is inherently consistent with the part geometry due to the use of a single fabrication machine. The primary disadvantage of this concept is the requirement of planar-like features (*i.e.* large radius of curvature) as cleaning off the excess conductor becomes user-intensive and thus prohibitive for smaller features. This limitation restricts this methodology for applying the stretchable conductors to wings with arbitrary topologies to the low-curvature outer surfaces unless augmented by other methods.

To highlight the possibility for the use of stretchable conductors on the inner surface of a wing with arbitrary topology, an alternative method of "tunneling" through rib-like features near the surface of the wing was introduced. A similar methodology to the channels was used where small straight tunnels were removed pre-print from the design of the underlying structure to allow direct wire channels through the load-bearing topology. This method allowed the stretchable conductor to be extruded through use of a syringe with a needle sufficient to extend the length of the conductor, as seen in Figure 5.

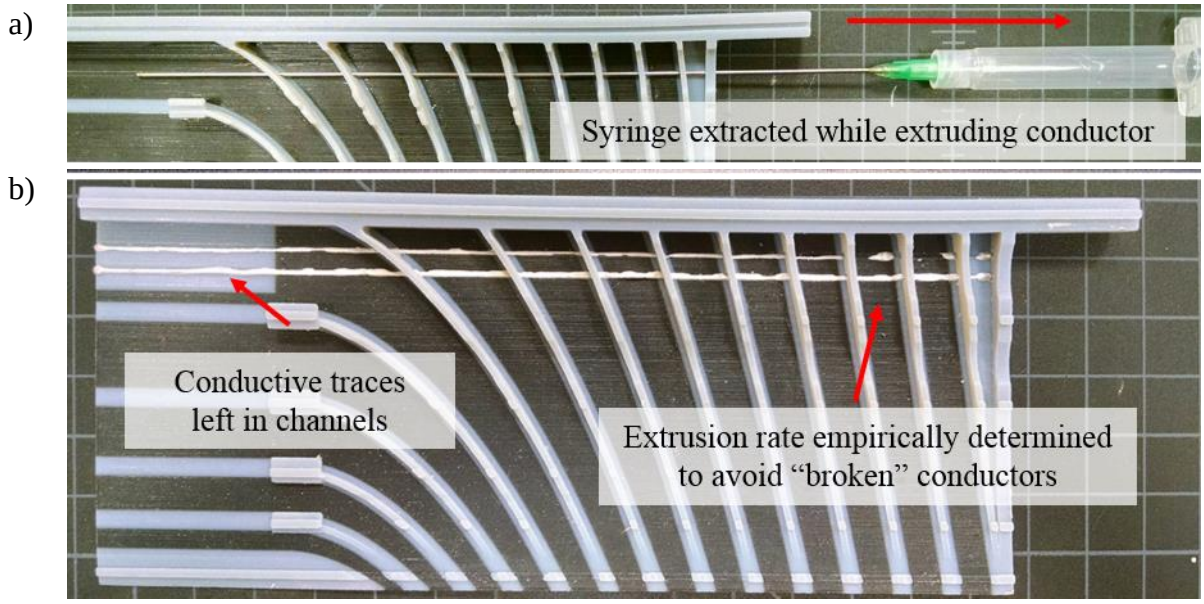

Figure 5: The channels through the topology were filled via
a) extrusion from a syringe that b) left conductive traces

As the syringe was removed, the conductor was deposited in the channel, eliminating the need of post-extrusion cleaning. The extrusion rate was empirically determined over a set of tests so as to avoid broken conductor paths while preventing overflow of the liquid from the channels post-cure. A large limitation of this methodology is that the extrusion of the conductor is then restricted to a straight line (by the nature of a straight needle). However, with the appropriate development of extrusion printing technologies, writing over arbitrary topology could be accomplished, eliminating the need to remove load-bearing structure for the conductor.

3 DEMONSTRATOR

To exemplify how these additive techniques could enable exploration of novel actuation and sensing mechanisms for aeroelastic testbeds, a table-top demonstrator was designed and constructed. Drawing from the ideas described above, the demonstrator leveraged these technologies into a trailing edge control surface with distributed sensing and actuation.

3.1 Integrated distributed sensing and actuation

A flow-sensing technique was desired that could be collocated with the deforming spines to investigate distributed flow measurement about the morphing trailing edge. Artificial Hair Sensors (AHS), as seen in the photo inset of Figure 6, were selected as a low-footprint, low-power sensor [10] that could enable such sensing within the mixed rigid-stretchable topology. Utilizing a common “mechanical island” technique from stretchable electronics, the AHS would be located along the low-strain spines of the control surface (seen in Figure 6) which would move under actuation, but not require the sensors to experience large strains. Given a suitable potting footprint these sensors would protrude from the trailing edge control surface into the flow, escaping the boundary layer, indicated in the illustrated inset of Figure 6.

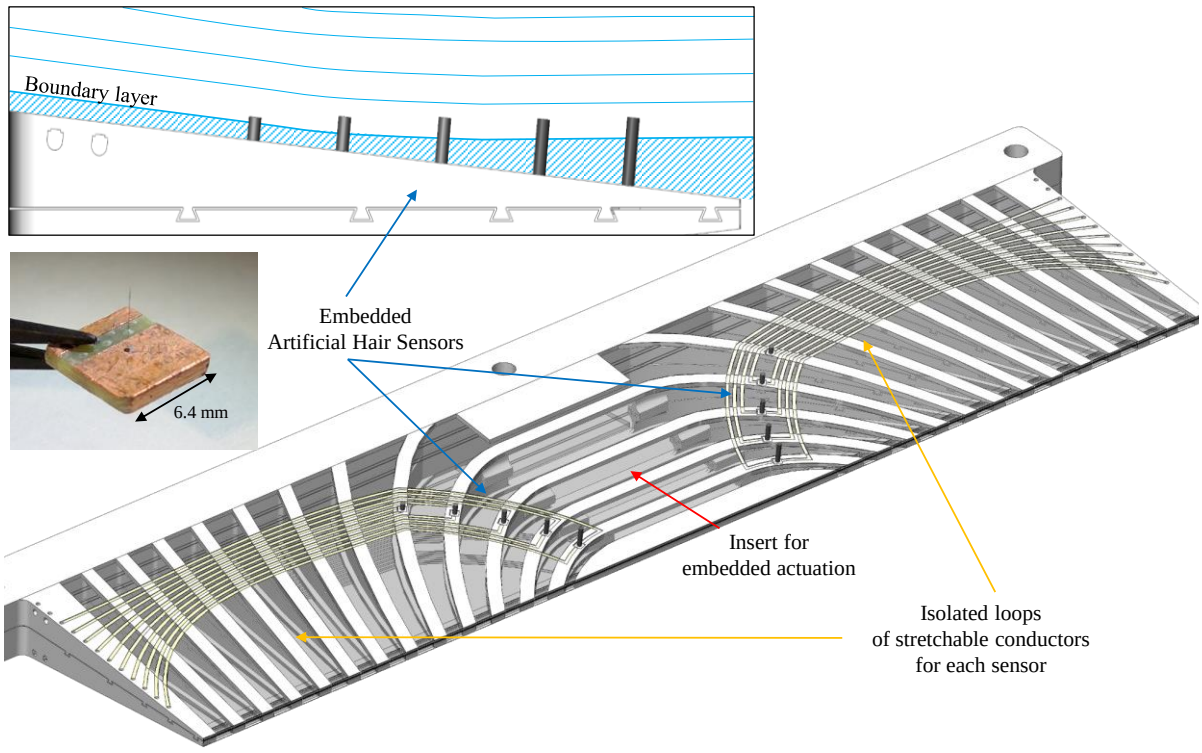

Figure 6: An overview of the demonstrator for Artificial Hair Sensor integration (hair diameter illustrated at 20x scale)

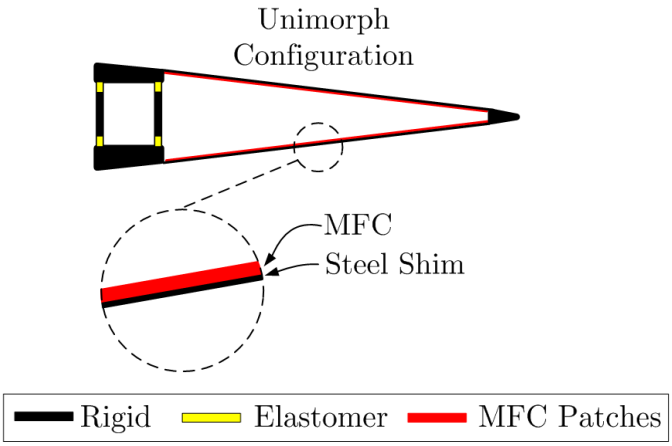

Figure 7: Actuation implementation (via Pankonien *et al.* 2014 [11])

These AHS would provide vertically-integrated flow forces to assess the morphing control surface's effectiveness on flow alteration. Note that although the other features in the figure are to scale, the hair sensors diameters have been amplified by 20x to be visible within the context of the geometry as the hair sensor diameter can be as small as 5 micrometers. As can be seen by the curved individual circuit loops within the demonstrator design, the wiring for the sensors could be selectively chosen to avoid high strain regions (such as near the trailing edge) without regard to the underlying topology. Additionally, sensors (or actuators) can be electronically isolated, as shown, or share connections to minimize wiring complexity.

Desiring a bending trailing edge to conform with the MELD boundary conditions, the bending Macro-Fiber Composite (MFC) unimorph scheme, shown in Figure 7, previously used in Pankonien *et al*. 2014 [11] was selected. This mechanism had the added benefit of utilizing high voltage but low current which would minimize the power dissipated in the stretchable circuitry. This design was realized as a MFC patch epoxied to a stainless steel shim on both the upper and lower surfaces of the structure, similar to the figure above.

3.2 Demonstrator as fabricated

Consistent with the use of Repeated Interpenetrating Fastening Features (RIFFs) by Pankonien *et al*. 2017 [5], the topology of the trailing edge was divided along the mid-plane with small dovetail-shaped cuts propogated spanwise, seen in the inset in Figure 6. This method permitted individual fabrication of the upper and lower surfaces without encompassing enclosed volumes or adding additional holes to the topology for support-material removal. Thus the upper and lower halves were printed on an Objet Connex 500 utilizing VeroWhite for the rigid structure and Tango Plus (a translucent elastomer for clarity) as the stretchable skin, as seen in Figure 8. Post support-removal via water-jet, the elastomer expanded slightly due to viscoelasticity in the material set, as seen in the figure. Ideally this effect would be reduced in the production of an actual wing-section as additional in-plane bending stiffness would be added fore of the rear spar.

a)

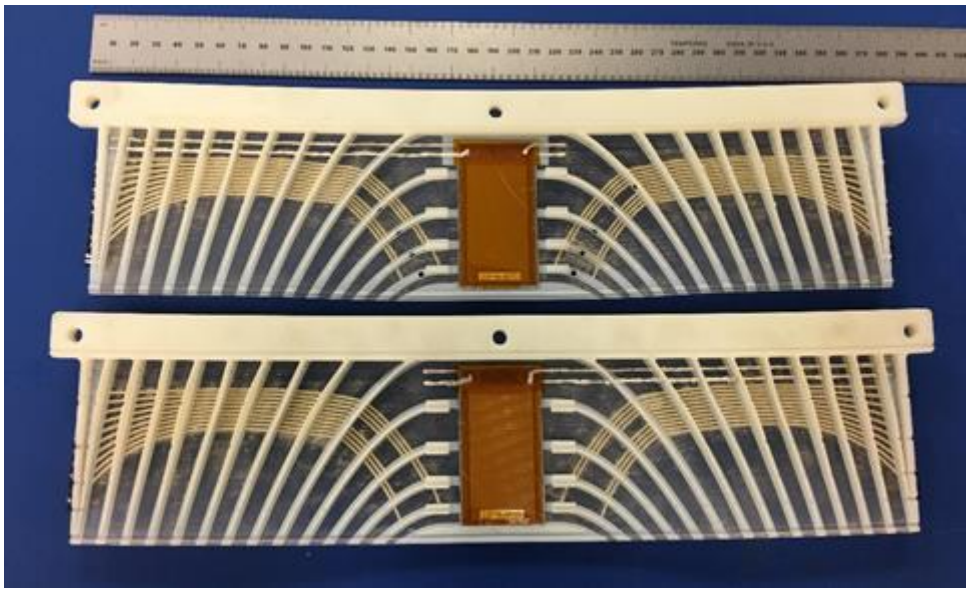

b)

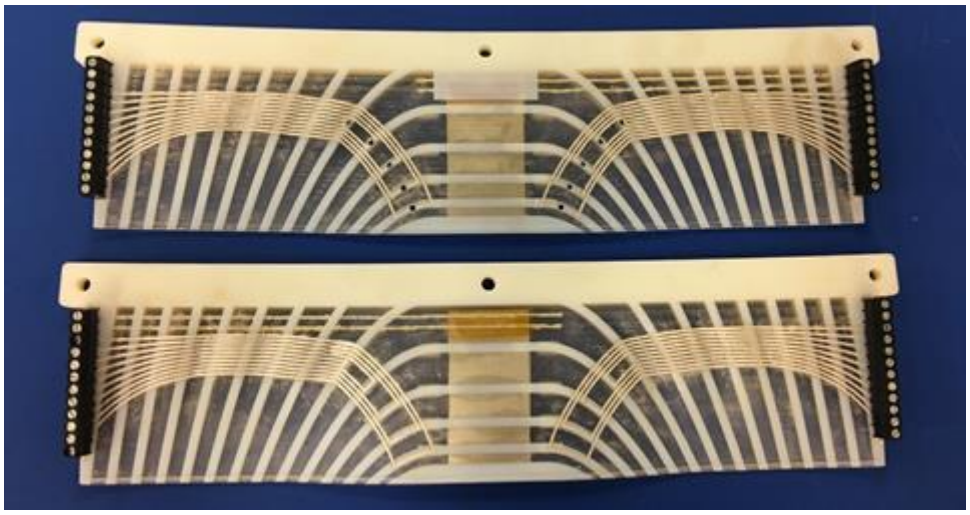

Figure 8: Both halves of the demonstrator shown from both
a) inside and b) outside

After printing and cleaning, stretchable conductor was cast on the outer surfaces of the upper and lower bodies, creating the stretchable conductive loops. Then, the inner conductor was extruded via syringe through small holes along the inner surface of the topology, providing wiring to the integrated actuator. Finally, the MFC unimorphs were glued to the inner surfaces and electrically connected to the stretchable conductor via additional conductive ink. Terminal blocks were added to pre-specified pin locations at the edge of the demonstrator to permit an interface with conventional wiring and diagnostic electronics.

The upper and lower halves were then pushed together in the thickness direction, permitting a snap-lock of the RIFFs to adhere the upper and lower surface together. The tolerance of this fit had been pre-selected to enable repeated attachment and detachment of the upper and lower halves during this investigation. For the purposes of demonstrators under aerodynamic loading, additional adhesive or fasteners could be required, with the RIFFs providing initial fastening for the upper and lower surfaces.

To illustrate the possibility for sensing, stand-ins for the Artificial Hair Sensors were printed and inserted within the holes to facilitate their observability within the demonstrator. However, these sensors were not transducers. So, to pictorially emphasize the stretchable conductors' ability to undergo large strains while maintaining conductivity, several LED sensors were also placed in the representative locations of the AHS, as seen in Figure 9. The morphing control surface was then actuated, showing smooth deformation from the kilovolt-actuated MFCs while simultaneously powering the LEDs. Additional loading illustrates the capability of the wiring to maintain conductivity under large compressive and tensile strains.

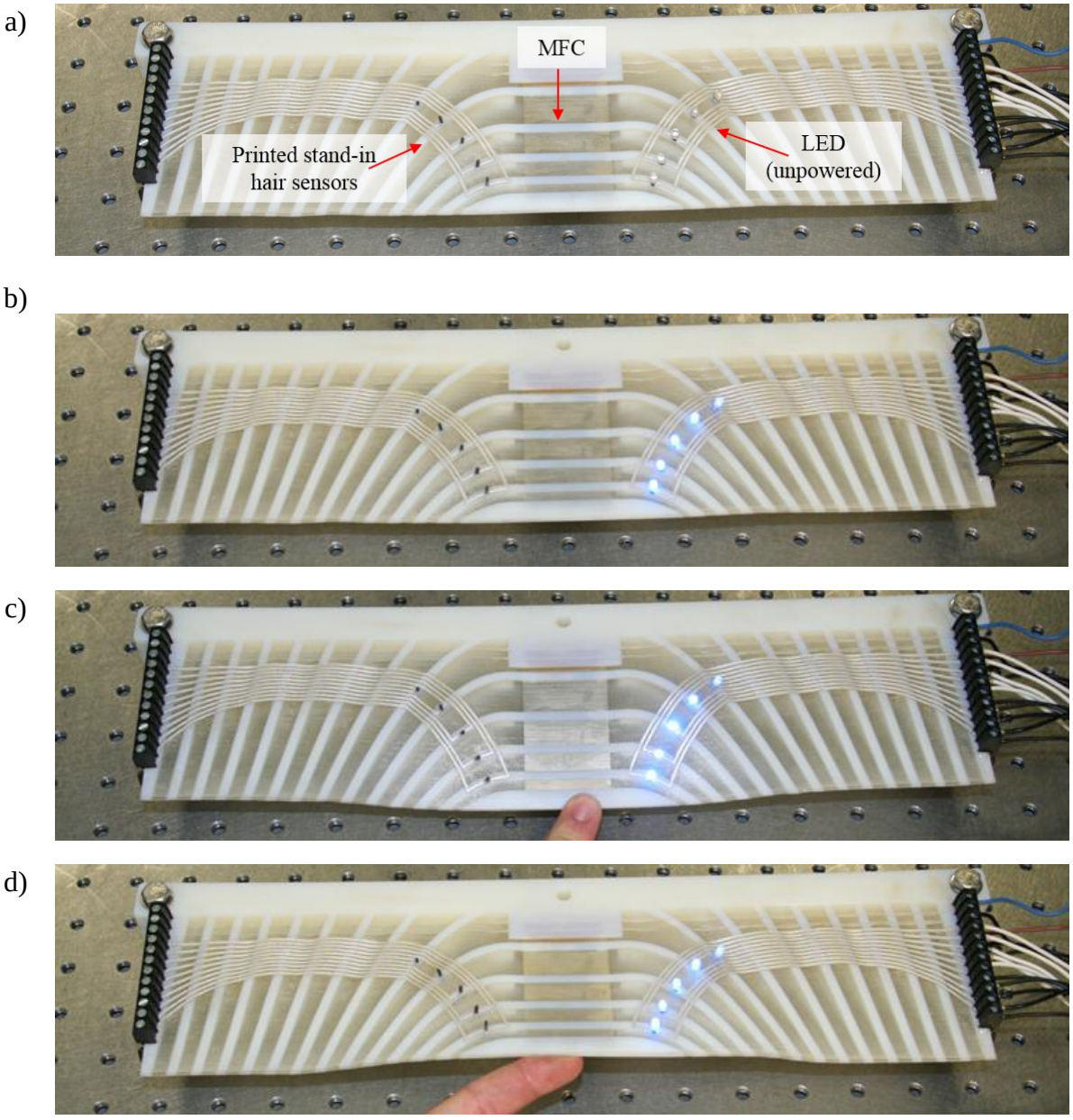

Figure 9: Demonstrator a) default position without power b) with powered "sensors" and actuator then further c) strained downward and d) upward with powered sensors to show the robustness of the circuitry.

While this demonstrator was constructed via additive techniques, there potentially exists a technique to construct a similar demonstrator with traditional subtractive techniques (such as CNC mill). However, an identical surface constructed using subtractive techniques would require at least 50 parts, which were printed in just 2 parts using additive manufacturing. Although difference in the number of parts is only one method of characterizing the ease of prototype manufacturing, a more in depth analysis is outside the scope of this work.

4 DISCUSSION OF IMPACT

4.1 Parametric variation in scripted geometry framework

Although this example of an additively-constructed morphing trailing edge highlights several production methodologies for independent control over stiffness and wiring locations, the design is motivated by the capability of this additive fabrication to rapidly realize non-conventional analysis-driven designs. To accomplish this rapid iteration, an appropriate framework for capturing the relevant topology for export to analysis and fabrication was needed. Accordingly, the geometry from the parameterization in Section 2.1 was converted into the open source Engineering Sketch Pad (ESP) for use within the Computational Aircraft Prototype Syntheses (CAPS) framework [12], where multi-fidelity optimization of aeroelastic vehicles has been implemented and demonstrated [13] to create the designs shown in Figure 10.

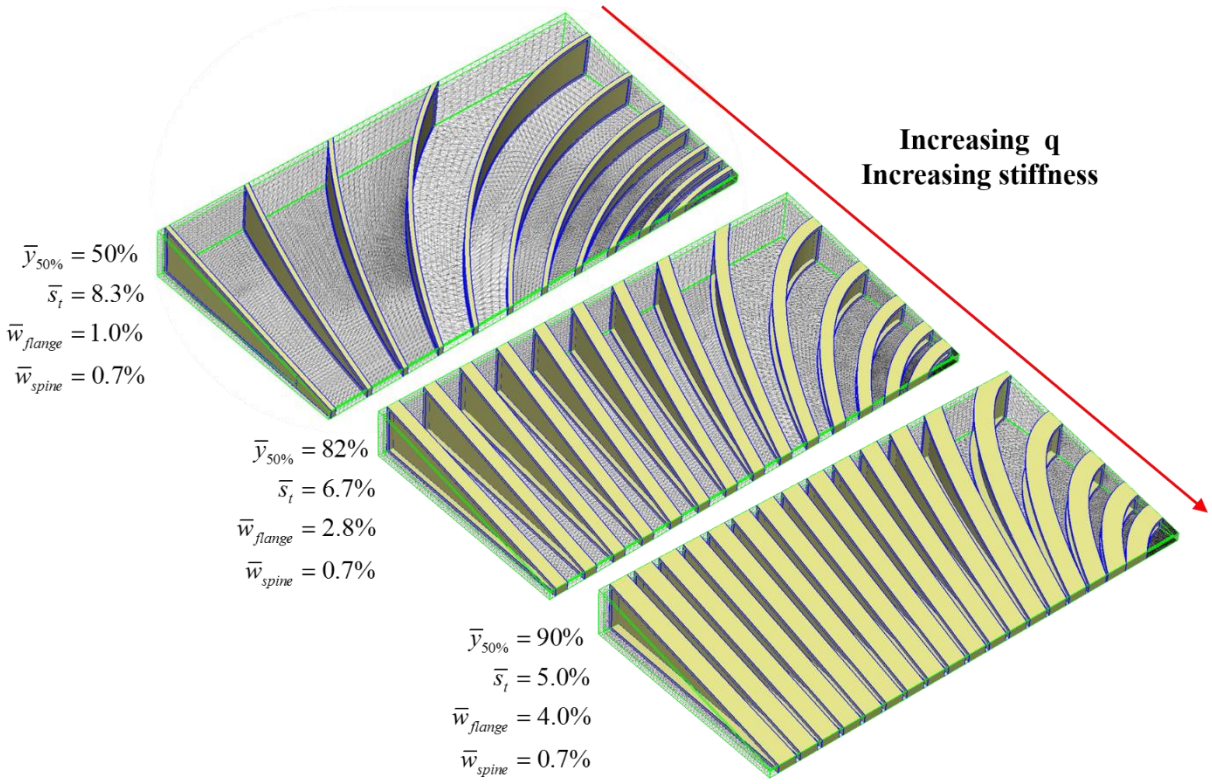

Figure 10: Changes in transition region are accomplished via scripted geometry generation while increasing notional operating dynamic pressure

The combination of low-parameter topology descriptions combined with a scripted geometry generation allows for rapid exploration of the design space to create intuitive topological solutions to complex requirements. For example, as seen in Figure 10, increasing stiffness of the morphing control surface design to accommodate increasing dynamic pressure is readily accomplished by altering the spine thickness, spacing, and turning parameter without altering material properties. Here the design parameters are nondimensionalized by the span of the transition region (*i.e.* l_t) for generality. These resultant designs, both as built-up element models and 3D topological meshes can be readily exported to aeroelastic analysis software for optimization and 3D-printers for fabrication, respectively.

The realization of the description of additively-constructible topologies such as these within a common framework for both fabrication and analysis highlights the tractability of this approach for reducing iteration time in experimentally validating complex, optimized designs. With the added flexibility of variations in material stiffness in addition to the geometry, a very large range of stiffnesses is possible even with constant mass.

4.2 Application to other problems

Although this work has primarily focused on a morphing trailing edge concept with specific instances of distributed actuation and sensing, the techniques are applicable to other desired morphing shapes. For example, the leading edge of a wing could be parameterized with a similar topology. Thus, an entire morphing airfoil could be joined about a single spar-like structure, and be produced via additive manufacturing. Furthermore, from a planform perspective, selectively introducing compliance through elastomer could allow for large planform changes without resulting in slider-surfaces.

Also importantly, the impact of the number or location of sensors and actuators on the internal topology has been minimized from an integration perspective. The devices utilized in the demonstrator have shown that if the actuators/sensors are completely electronic they can be individually collocated with desired measurement sites. This development is unique to traditional flow sensing technology (such as pressure tubes) or even hot-film sensors that might not be compatible with stretchable surfaces or isolated spines. The use of only a single machine for consistency within this fabrication process should also not be underestimated for reducing the iteration time in design changes.

Finally, although this work has focused primarily on the geometry of the control surface as a guiding principle for stiffness control, the alternating use of “hard” and “soft” plastic should indicate to the reader that the performance of the trailing edge is not solely dependent on geometry, but also material stiffness. The capability of multi-material 3D-printers to selectively alter material stiffness over a wide range of material properties while maintaining the same overall geometry and mass further motivates investigation of testbeds in this domain with identical geometries and mass distributions, but radically different stiffness properties. Leveraging such capabilities in the context of aeroelastic testbeds has wide applicability towards increased independence of mode shapes from geometry and mass distribution, which is exactly the inverse of typical aeroelastic testbed fabrication techniques.

5 CONCLUSIONS

Additive fabrication of a complex structural topology described by a limited parameter set with application to aeroelastic testbeds has been illustrated via the production of a morphing trailing edge control surface with integrated yet distributed actuation and sensing. This demonstrator was developed by reinterpreting an existing morphing trailing edge concept, the MELD, within the context of multi-material 3D printing. This method eliminated the exclusively geometrically-driven compliant mechanism while enabling the integrated fabrication of both stretchable skin and compliant load-carrying structure. The simultaneous production of both skin and structure enabled high-precision positioning of channels within the skin that were also consistent with the underlying structure. When combined with a straightforward casting methodology, these channels formed integrated stretchable conductors. These conductors enabled independence of wiring from the underlying topology while eliminating the stiffness and nonlinear contact problems typical of wiring within a complex morphing structure.

The relevance of these methods was embodied via the fabrication of a table-top morphing demonstrator. The demonstrator illustrated how distributed sensing and actuation methodologies could be enabled for the measurement of separating flow co-located with distributed shape change (morphing). The application of these computer-driven additive fabrication methods towards the validation of analysis-driven optimization was indicated via the production of several geometric variations of the control surface with varied stiffnesses via the CAPS framework. These results identify an exciting new approach to fabricating aeroelastic and dynamic structures where the stiffness and mass distributions of complex geometries can be nearly independently specified, while maintaining tractability within a high-fidelity analysis framework. These fabrication and analysis methods can then be combined to realize optimized high-performance morphing aeroelastic testbeds.

6 ACKNOWLEDGEMENTS

The first author gratefully acknowledges the funding of the National Research Council - Research Associate's Program for its funding of the research. This work has been cleared for public release – case number 88ABW-2017-2533.

7 REFERENCES

[1] Liu, R., Wang, Z., Sparks, T., Liou, F., and Newkirk, J., *Aerospace applications of laser additive manufacturing*, in *Laser Additive Manufacturing: Materials, Design, Technologies, and Applications*, pp. 351–371 (2016) [DOI:10.1016/B978-0-08-100433-3.00013-0].

[2] Hartl, D.J., Reich, G.W., and Beran, P.S., "Additive topological optimization of muscular-skeletal structures via genetic L-system programming," in *24th AIAA/AHS Adaptive Structures Conference* (2016).

[3] Hobeck, J.D., Laurant, C.M.V., and Inman, D.J., "3D printing of metastructures for passive broadband vibration suppression," in *20th International Conference on Composite Materials, Denmark, Copenhagen* (2015).

[4] Shkarayev, S.V., Ifju, P.G., Kellogg, J.C., and Mueller, T.J., "Flexible-Wing Micro Air Vehicles, Introduction to the Design of Fixed-Wing Micro Air Vehicles Including Three Case Studies," *AIAA Education Series*, 186–240 (2006) [DOI:10.2514/5.9781600862106.0185.0240].

[5] Pankonien, A.M., Reich, G.W., Schottelkotte, J.J., Lindsley, N., and Smyers, B.M., "3D-Printed Wind Tunnel Flutter Model," 2017, 58th AIAA/ASCE/AHS/ASC Structures, Structural Dynamics, and Materials Conference, AIAA SciTech Forum.
[6] Campbell, I., Bourell, D., and Gibson, I., "Additive manufacturing: rapid prototyping comes of age," *Rapid Prototyping Journal* **18**(4), 255–258 (2012) [DOI:10.1108/13552541211231563].
[7] Woods, B.K.S., Parsons, L., Coles, A.B., Fincham, J.H.S., and Friswell, M.I., "Morphing elastically lofted transition for active camber control surfaces," *Aerospace Science and Technology* **55**, 439–448 (2016) [DOI:10.1016/j.ast.2016.06.017].
[8] Woods, B.K.S., and Friswell, M.I., "Multi-objective geometry optimization of the Fish Bone Active Camber morphing airfoil," *Journal of Intelligent Material Systems and Structures* **27**(6), 808–819 (2015) [DOI:10.1177/1045389X15604231].
[9] Locatelli, D., Mulani, S.B., and Kapania, R.K., "Wing-box weight optimization using curvilinear spars and ribs (SpaRibs)," *Journal of Aircraft* **48**(5), 1671–1684 (2011) [DOI:10.2514/1.C031336].
[10] Phillips, D.M., Ray, C.W., Hagen, B.J., Su, W., Baur, J.W., and Reich, G.W., "Detection of flow separation and stagnation points using artificial hair sensors," *Smart Materials and Structures* **24**(11) (2015) [DOI:10.1088/0964-1726/24/11/115026].
[11] Pankonien, A.M., and Inman, D.J., "Aeroelastic performance evaluation of a flexure box morphing airfoil concept," in *Proceedings of SPIE - The International Society for Optical Engineering* **9057** (2014) [DOI:10.1117/12.2046406].
[12] Alyanak, E., Durscher, R., Haimes, R., Dannenhoffer, J., Bhagat, N., and Allison, D., "Multi-fidelity Geometry-centric Multi-disciplinary Analysis for Design," in *AIAA Modeling and Simulation Technologies Conference, AIAA Aviation Forum* (2016) [DOI:10.2514/6.2016-4007].
[13] Bryson, D.E., Rumpfkeil, M.P., and Durscher, R.J., "Framework for Multifidelity Aeroelastic Vehicle Design Optimization," in *AIAA Aviation 2017* (2017).

COPYRIGHT STATEMENT